Surface & Coatings Technology xxx (2015) xxx–xxx

Contents lists available at ScienceDirect

Surface & Coatings Technology

journal homepage: www.elsevier.com/locate/surfcoat

Evaluation and characterisation of urinary catheter coating utilising Hansen solubility parameters and FEA analysis

Brendan J. Carberry, Joseph Farrell, James E. Kennedy *

Centre for Industrial Services and Design, Athlone Institute of Technology, Athlone, Co. Westmeath, Ireland

ARTICLE INFO

Article history:
Received 20 February 2015
Revised 12 June 2015
Accepted in revised form 16 June 2015
Available online xxxx

Keywords:
Hansen solubility parameters
Tea's diagram
Solvent blends
Contact angle
FEA

ABSTRACT

This work investigated the Hansen solubility parameters required to optimise a functional polyurethane base coat as an attachment for a lubricious polyvinyl pyrrolidone coating for polyvinyl chloride urinary catheters. Solvents included benzyl alcohol, tetrahydrofuran, acetonitrile, and cyclohexanone and blends thereof. The viscosity of the polymer–solvent compositions was characterised using Redwood No.1 viscometer. The UV cured polymer–solvent blends were fully characterised using scanning electron microscopy, differential scanning calorimetry, and digital goniometry. A finite element analysis (FEA) model of the urethra during catheterisation was also developed to illustrate the magnitude of deflection expected with the hydrophilic coating on the catheter. Based on the theoretical modelling and subsequent experimental results this demonstrated that the materials dissolved in short succession of immersion in the calculated solvent blend. Also, the various compositions of polyvinyl pyrrolidone in the solutions produced noticeable variations in coating thicknesses ranging from 8 μm to 26 μm.

1. Introduction

Indwelling bladder catheters and ureteral stents restore essential functions that have been lost as a result of trauma, disease or ageing. The challenge is to produce a coating in which the antibacterial activity persists for the lifetime of the device, which is not reduced by contact with urine, has a broad spectrum of activity and does not select for and spread bacterial resistance to antimicrobials [1]. In this regard, a hydrophilic coating on the catheter can replace or supplement the lubricating action of the endothelial surface layer [2], while also facilitating catheterisation [3]. Looking towards the medical device sector in particular catheter manufacturing; where the application of biomaterials such as hydrophilic coatings is essential to increase biocompatibility [4], reduce biofilm formations [5] and most importantly to increase comfort for the patient when introducing the catheter into the body or in this instance the urethra. Traditionally short-term catheters are composed of plasticised polyvinyl chloride (PVC). PVC is a material of enormous technical and economic importance. It stands second in the world after polyethylene as regards the production and consumption of a synthetic material [6]. However, these materials can have a high coefficient of friction, which makes insertion into the body difficult. In this regard, self-lubricating PVC catheters with a hydrophilic coating are becoming increasingly popular, especially for intermittent catheterisation, because of the greater ease of passage and decreased trauma and discomfort [7]. These coatings have a low friction coefficient when wet and typically comprise hydrophilic polymers such as polyvinyl pyrrolidone (PVP). PVP is a hydrophilic polymer with a time dependant low contact angle of approximately 56° after initial contact with surface [8]. It is for this reason, and the possibility of hydrogen bonding with bodily fluids [9], that PVP is used as a biomaterial coating on standard PVC catheter substrate material.

Urinary tract infections (UTIs) are one of the most common bacterial infections, particularly in women of all ages; however, as age increases the prevalence of UTIs increases [10]. Where UTI in men younger than 45 years is usually not associated with significant structural or functional urinary tract abnormalities [11], however, elderly men have been found to be more prevalent with UTIs due to urological abnormalities [12]. Despite statistics showing 70% of women are more vulnerable to UTIs then men, during the first year of life the ratio is more 50:50 [12]. In most children UTIs are isolated acute infections and recovery is typically very fast, but in a small majority of children UTIs progress leading to alternative care requirements like catheterisation. Urinary catheters are used to treat patients with urine retention; however this artificial surface in the presence of tissue acts as an anchoring point, hence facilitates adhesion of bacteria which commonly forms a biofilm when used as a long term implant. Biofilms are a predominant microorganism form of life present in any hydrated biologic system [13]. In the human body, the biofilm bacteria are protected against antibiotic treatment and the immunity system [14]. These biofilms are capable of propagating the whole length of the catheter to all areas of the urinary system. If this happens the urinary tract infection will worsen, and this is then known as a catheter-associated urinary tract infection (CAUTI). CAUTIs

* Corresponding author.
E-mail address: jkennedy@ait.ie (J.E. Kennedy).

http://dx.doi.org/10.1016/j.surfcoat.2015.06.029
0257-8972/

are the most common type of nosocomial infection and account for over 1 million cases annually [15]. To put this in to perspective, indwelling urinary catheters are placed in up to 25% of hospitalized patients and are a leading cause of hospital-acquired infection [16]. It has been verified through in-vivo studies that hydrophilic coated catheters perform better than uncoated catheters with regard to haematuria and preference [7].

To this end, the manner in which the solvents and solvent blends are synthesised so that selected polymers can be adequately dissolved prior to the coating process is not readily discussed. Therefore, applying the theory of "*likes dissolve likes*" [17] allows for the solvent Hansen solubility parameters to be quantitatively matched to that of the polymers in order to evaluate how effective they are at producing a useable homogenous coating solution. The individual solvent compositions were purely quantified from a tertiary diagram, known as a Tea's diagram, presenting the fractional dispersion forces (F δd), the fractional hydrogen forces (F δh), and the fractional polar forces (F δp), i.e., the cohesive energy of the solvents. Based on the characterisation results, some interesting findings are discussed and the Hansen solubility parameter polymer–solvent synthesis technique is proposed.

2. Materials and methods

2.1. Materials and curing methods

The thermoplastic polyurethane (TPU) was provided by the Centre for Industrial Services and Design (CISD), Athlone, Ireland in resin form with the trade name Estane 5715P. The PVP K90 (360,000 MW) was supplied by CISD with the trade name Sigma Aldrich. The solvents benzyl alcohol, tetrahydrofuran, acetonitrile, and cyclohexanone were supplied by the CISD with the trade names Merck, AppliChem, and Lab-Scan. In this study, the various PVP compositions ranging from 2 g to 7 g were dissolved in 100 g of a solvent blend calculated from the Hansen solubility parameters. The TPU base coat was applied by dipping and was cured by using the thermal chamber to evaporate the solvents away. The PVP coating curing methods were carried out in two steps, first the thermal chamber was used to evaporate the solvents at 75 °C for 20 min leaving only the thin polymer coating behind. Secondly was the UV-irradiation which was carried out on the Dr. Groebel unit. The UV-irradiation was used to crosslink the PVP and the times varied between 5 and 15 min and 30 W/m^2.

2.2. Polymer–solvent viscosity

The apparatus used to determine the polymer–solvent viscosity was the Redwood No.1. Each of the samples was repeated in triplicate and their average results were used. The reservoir of polymer–solvent solution was maintained at room temperature and the volume of the solution to be displaced was 50 ml (see Table 2.1). In order to determine the kinematic viscosity (V) the system constants A and B were taken to be 0.247 and 65 respectively with Eq. (1), where t is the time required to displace the 50 ml.

$$V = At - \frac{B}{t} \quad (1)$$

Table 2.1
Polymer–solvent coating parameters.

Coating No.	PVP [g]	Optimal solvent blend calculated from Eqs. (2)–(9)	UV cure time [min]
1B	2	36%, 24%, 24%, and 16% of tetrahydrofuran, cyclohexanone, benzyl alcohol, and acetonitrile respectively	5
2B	2		15
3B	3		5
4B	3		15
5B	4		5
6B	4		15
7B	5		5
8B	5		15
9B	7		15

2.3. Coating thickness characterisation

The cured coated intermittent catheters with the PVP coating were prepared by freezing sections of 1 cm long with liquid nitrogen and cutting them as small samples. These samples were then gold plated to enhance the surface features during the SEM analysis. The SEM analysis was magnified between 50 and 100 μm to accurately differentiate and measure the coating thickness relative to the catheter.

2.4. Coating contact angle

The uncoated and coated catheters were cut into sections of 3 cm long, opened-out and spread on a flat surface in front of the camera lens. The sessile drop was of a distilled water and was volumetrically maintained consistently at approximately 0.002 ml for all samples (average of ten samples tested). Each study was conducted for a duration of 60 s in order to evaluate any change in contact angle over time. The apparatus used consists of the Logitech QuickCam Pro 4000, and the PC analysis software package is named Fta1000.

2.5. Coating coefficient of friction

The coated catheters were placed in a water bath at 37 °C with a pH. of 6.6, approximately that of the urethra in a healthy body. The friction jig is a mechanical apparatus with variable loading (compressive) capability; the loading for this study was kept constant at 3.924 N. A Lloyd cyclic tensile tester was used to push and pull the hydrophilic coated catheter through the friction jig. This was repeated for 50 cycles. This was a comparative study of the coating coefficient of friction vs. the uncoated catheter coefficient of friction. The pads used on the friction jig were a silicone material, the material selection to measure the coefficient of friction against has a great influence on final results since friction is not an independent value.

2.6. FEA model of urethra

The urethra was modelled as a solid hollow cylinder with an inner radius of 1 mm and an outer radius of 20 mm, this was extruded at 100 mm in length, and the catheter was modelled as a shell of 200 mm long with a 20 mm taper to a 0.5 mm round tip. The urethra material properties were based on the Arruda–Boyce constitutive hyperelastic equation [20] where the constants $\mu_0 = 33$KPa, $\lambda_m = 1.001$, and $D = 1E^{-8}$ were used.

3. Theory/calculation

3.1. Hansen solubility parameters

The total energy of evaporation is equal to the total cohesive energy (E), which is the energy required to break all the cohesive bonds. The cohesive energy of a polymer or solvent can be fully quantified as a variation of the dispersion cohesive energies (E_D), the polar cohesive energies (E_P), and the hydrogen bond cohesive energies (E_H). The Hansen solubility parameter accounts for all these energies and can be quantitatively defined by Eq. (2).

$$E = E_D + E_P + E_H \quad (2)$$

However, a more conventional approach is to express the total energy in terms of the cohesive density, this is done by dividing each constituent by the molar volume as shown in Eq. (3).

$$\frac{E}{V} = \frac{E_D}{V} + \frac{E_P}{V} + \frac{E_H}{V} \tag{3}$$

This can be represented in the reoccurring format associated with the solubility parameter which both Hildebrand and Hansen comply to.

$$\delta^2 = {\delta_D}^2 + {\delta_P}^2 + {\delta_H}^2 \tag{4}$$

The solubility parameters which include the interaction radius (R_a), were replicated from the Hansen solubility parameters handbook [18], and can be seen in Table 3.1. The interaction radius value was used as a benchmark to determine whether or not the solvent blend would dissolve the polymer materials. Since the coating of the PVC catheters was done in two steps; a basecoat of TPU followed by a PVP topcoat, a solvent blend was synthesised to accommodate the interaction radii form both polymers. Hence, a single solvent blend was used in separate instances to create two coatings solutions. Therefore, by using Eq. (5) the theoretical interaction radius was determined; if the theoretical interaction radius was higher than the referenced interaction radius it was likely the polymer would not dissolve in the solvent blend.

$$R_a = \sqrt{4(\delta_{D1} - \delta_{D2})^2 + (\delta_{P1} - \delta_{P2})^2 + (\delta_{H1} - \delta_{H2})^2} \tag{5}$$

where the subscripts D, P, and H, represent the dispersion, the polar, and the hydrogen energy densities respectively. The subscripts 1 and 2 are in relation to the polymer and the solvent respectively.

The adage "*likes dissolve likes*" is fully exploited in the tertiary diagram known as the Tea's diagram. The Tea's diagram is a convenient way to depict the relative strengths of the three forces; more-so, the diagram is very good at predicting solvent blend ratios which otherwise individually may not have the potential to dissolve a certain material.

The solvent and polymer intermolecular forces were presented on a Tea's diagram with each axis a scale of 0 to 0.1 (0%–100%). Therefore, to achieve this the intermolecular forces were taken as the fractional dispersion cohesive energy densities (f_D), the fractional polar cohesive energy densities (f_P), and the fractional hydrogen bonding cohesive energy densities (f_H). Eqs. (6)–(8) represent these fractional forces f_D, f_P, and f_H respectively.

$$f_D = \frac{100\ (\delta_D)}{(\delta_D + \delta_P + \delta_H)} \tag{6}$$

$$f_P = \frac{100\ (\delta_P)}{(\delta_D + \delta_P + \delta_H)} \tag{7}$$

$$f_H = \frac{100\ (\delta_H)}{(\delta_D + \delta_P + \delta_H)} \tag{8}$$

Table 3.1
Hansen solubility parameters for selected materials.

Material	δD [MPa$^{1/2}$]	δP [MPa$^{1/2}$]	δH [MPa$^{1/2}$]	R_a [−]
Benzyl alcohol (●)	18.4	6.3	13.7	–
Cyclohexane (●)	16.8	0	0.2	–
Acetonitrile (●)	15.3	18	6.1	–
Tetrahydrofuran (●)	16.8	5.7	8	–
Polyvinyl chloride (PVC) (●)	19.2	7.9	3.4	6
Polyvinyl pyrrolidone (PVP) (●)	17.5	8	15	14
Polyurethane (TPU) (●)	18.1	9.3	4.5	8

For any solvent blend or polymer–solvent system, Eq. (9) must be true in order for the materials to be thermodynamically stable [19]:

$$f_H + f_P + f_D = 100. \tag{9}$$

The quantities of the PVP polymer to be added to the solvent blend range from 2 g, 3 g, 4 g, 5 g, and 7 g. The purpose of the various loadings of PVP K90 in the solvent blend was to evaluate the performance of the polymer–solvent system through the stated characterisation methods.

4. Results and discussion

4.1. Tea's diagram

As presented in the Tea's diagram in Fig. 4.1, the interaction radius of both the TPU and PVP falls inside the solvent blend interaction line, and this is represented by a continuous red line. This indicates that these two materials will dissolve in a solvent blend over a given period of time. With regard to the black rings, these highlight the interaction radius limits of the polymer materials. The bottom axis of the diagram in Fig. 4.1 is the fractional polar forces, the right axis is the fractional hydrogen forces, and the left axis is the fractional dispersion forces, as calculated using Eqs. (2)–(9). It was found that a blend of 2 or more solvents (tetrahydrofuran, cyclohexanone, benzyl alcohol, and acetonitrile) provided the formulation capable of dissolving both the PVP and TPU within 15 min. Working within the Tea's diagram, the blend containing 36%, 24%, 24%, and 16% of tetrahydrofuran, cyclohexanone, benzyl alcohol, and acetonitrile yielded the optimal solvent parameters (known herein as the solvent system). From Eq. (5), the interaction distances were calculated and the corresponding values of 6.071, 4.5551, and 8.0388, for PVC, TPU, and PVP were on or below the associated R_a values as presented in Table 3.1. This indicated that the interaction radius containing 2–7 g of PVP by weight dissolved in 100 g of the solvent blend in less than 1 min, 5 g of TPU dissolved in approximately 15 min, and 5 g of the PVC took 4 h to show signs of cracking. In all experiments the solvent blends were maintained at room temperature, 18 °C ± 2 °C. These results prove that the Tea's diagram in conjunction

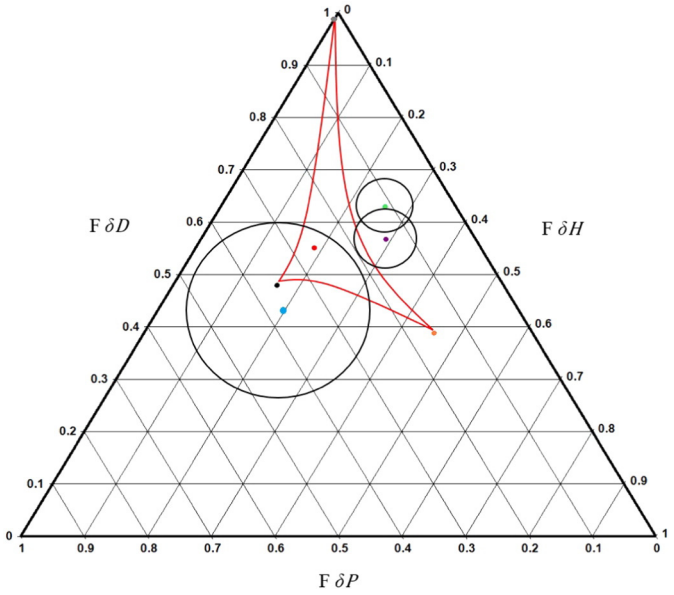

Fig. 4.1. Tea's diagram for polymer–solvent system including the polymers PVP, PVC, and TPU, and the solvents benzyl alcohol, tetrahydrofuran, acetonitrile, and cyclohexanone.

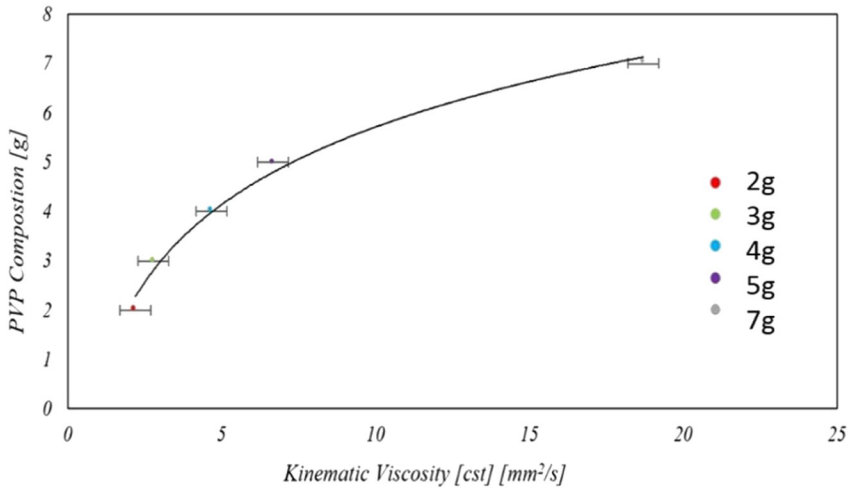

Fig. 4.2. PVP composition as a function of the kinematic viscosity.

with the Hansen solubility parameters generated a predictable model for designing an optimal polymer coating system.

4.2. PVP–solvent viscosity

After evaluating the viscosity of the PVP–solvent solution at 18°C(±2°C), the viscosity of a 2 g PVP solution in 100 g (by weight) of the solvent was 2.2cst ± 0.5cst, this increased exponentially to 18.7cst ± 0.5cst for the 7 g PVP composition solution (Fig. 4.2).

This increase is concentration dependent and the exponential growth can be attributed to the increased time the solution was present within the instrument. To confirm this, the change in kinematic viscosity with increasing PVP composition as a function of time was investigated. With regard to Fig. 4.3, this represents the Redwood seconds as a function of the kinemtic viscosity. The Redwood seconds can be defined as the time required for the 50 ml of polymer–solvent solution to pass through the viscometer orifice (∅ 1.62 mm). Looking at the % differences between the samples, and working from the base value of 2 g which took 54 s to pass through the orifice, the PVP concentrations of 3, 4, 5 and 7 g yielded percentage increases of 26, 111, 202 and 748% respectively. This increase can be attributed to the diameter of the orifice causing a reduction in flow due to the increased concentration of polymer molecules trying to get through the die length of the orifice. Considering that there was no induced shear pseudoplastic behaviour was not evident.

4.3. Coating thickness

It was found from the SEM imaging (Fig. 4.4) that the coating composition had a direct relationship on the coating thickness. The lowest concentration of UV cured PVP (2 g) solution onto the TPU coated PVC catheter resulted in a coating with a thickness of 8.08 μm. For the samples containing the 3 g, 4 g, 5 g, and 7 g PVP compositions these yielded thickness values of 10.51 μm, 15.78 μm, 21.65 μm, and 26.20 μm respectively. From the SEM images it can be seen the adherence of the coating to the catheter substrate is consistent and the coating is uniformly spread over the surface. No degradation was evident on the catheter surface which is primarily due to the solvent systems used in the coating solution, as predicted by the Tea's diagram (Fig. 4.1). However, the rough ends on the catheter from some images are a result of sample preparation.

4.4. Digital goniometry

From the contact angle analysis which was repeated in triplicate and averaged over a 10 day period. A value of 72.85° (Fig. 4.5) was found for the PVC catheter. The contact angle of PVP was lower than PVC and it reduced over time; this is expected from a hydrophilic polymer and can be seen in Fig. 4.6, the fitting was performed under the scatter with smooth lines function in Microsoft Excel.

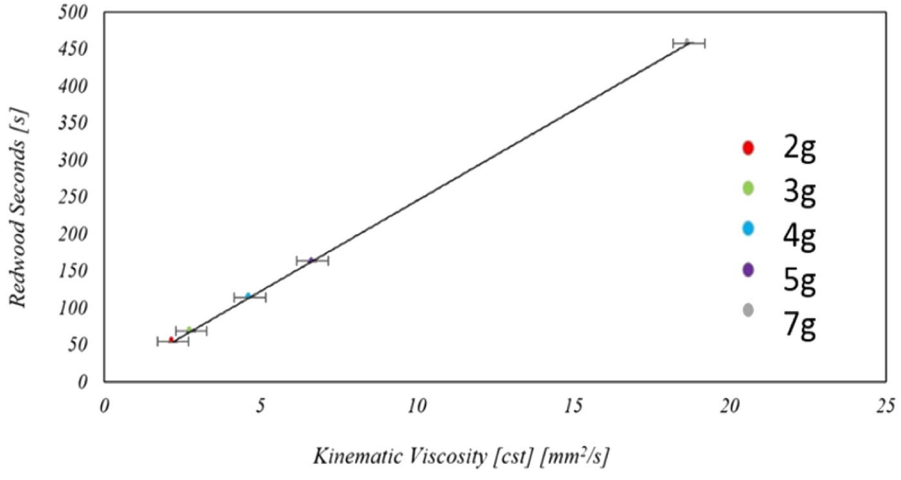

Fig. 4.3. Redwood seconds as a function of the kinematic viscosity for varying PVP solutions.

Please cite this article as: B.J. Carberry, et al., Surf. Coat. Technol. (2015), http://dx.doi.org/10.1016/j.surfcoat.2015.06.029

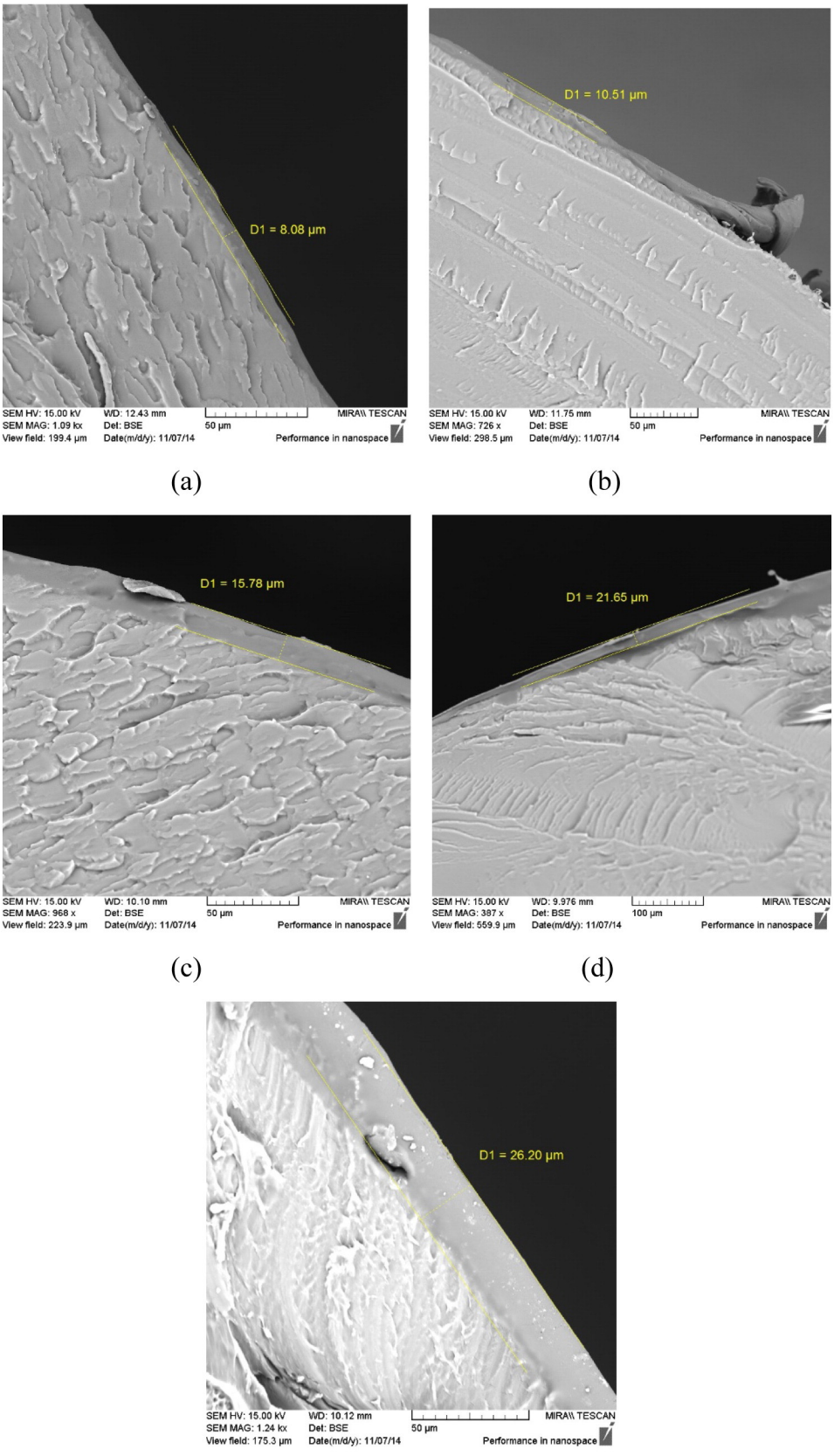

Fig. 4.4. SEM images; (a) 2 g PVP, (b) 3 g PVP, (c) 4 g PVP, (d) 5 g PVP, and (e) 7 g PVP concentration.

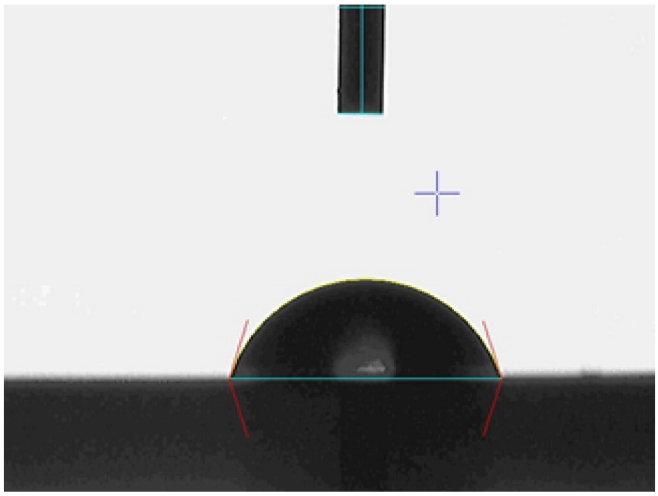

Fig. 4.5. Contact angle of the PVC catheter.

From Fig. 4.6 it can be seen the contact angle has come to a point where the rate of change of the contact angle is reducing greatly. This implies the peak is the final value of the surface contact angle. Hence, after 40 s the surface contact angle reduces to 28.05°. This time dependant contact correlates to the findings of Guo et al. [21], they found the final contact angle to be approximately 26.8° when evaluating PVP based polymers.

4.5. Coating coefficient of friction (CoF)

From the friction analysis of the PVP coated PVC catheters it was found that each of the PVP composition solutions provided a significant reduction in surface friction. The uncoated catheter under a compressive force between silicone pads yielded a coefficient of friction of approximately 0.4597 and the lowest coefficient of friction was observed from the 3 g PVP/solvent system coating with a value of approximately 0.0702. Therefore, the optimum coating provides a 6.55 fold reduction in surface friction in comparison to the uncoated catheter. Fig. 4.7 presents a bar chart of the various coated catheters relative to the uncoated catheter.

Since all the coatings showed sufficient durability, the CoF was the most important parameter to obtain. The reason for the variation in the coating CoF is due to the thickness of the layer. In theory, the thicker the layer the more the coating will swell, hence the more lubricous it will be with a lower CoF. However, this is not the case and form the results it can be seen a certain composition of PVP yields the lowest CoF. The reason for the higher CoF with the higher composition coatings of PVP is simply down to the fact the coatings were swelling too much. This led to clumping and fouling of the coating, hence increasing the CoF by providing obstructions between the catheter and the silicon pads on the friction jig.

Hence, the optimum coating from the view of durability and CoF, is coating 3B. Coating 4B is relatively close also, the only difference in the processing between these two coatings is 3B has 5 min UV irradiation, and coating 4B has received 15 min UV-irradiation. Non-the less, based on a number of repeated tests (50 cycles) there was a constant similar response from the coatings.

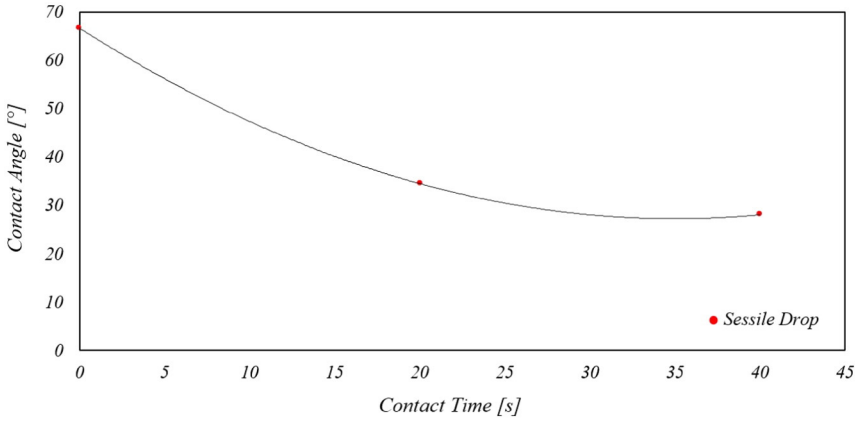

Fig. 4.6. Contact angle of the PVP coatings 66.65°, 34.50°, and 28.05° after 0 s (a), 20 s (b), and 40 s (c) respectively.

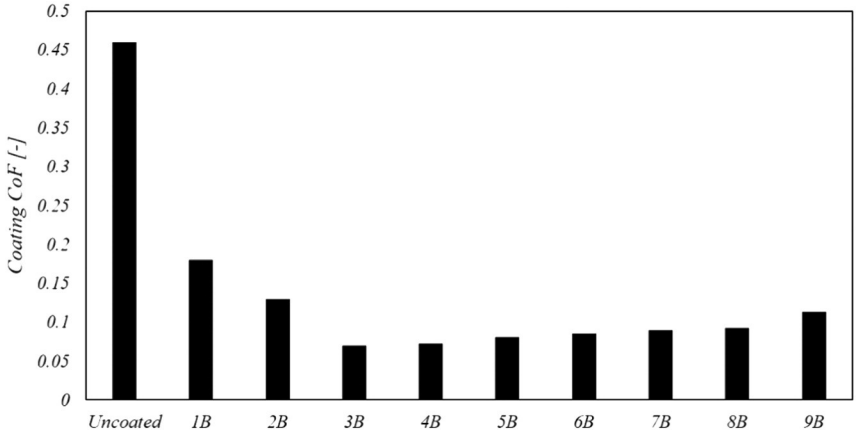

Fig. 4.7. Coefficient of friction of various PVP coatings relative to the uncoated catheter.

Please cite this article as: B.J. Carberry, et al., Surf. Coat. Technol. (2015), http://dx.doi.org/10.1016/j.surfcoat.2015.06.029

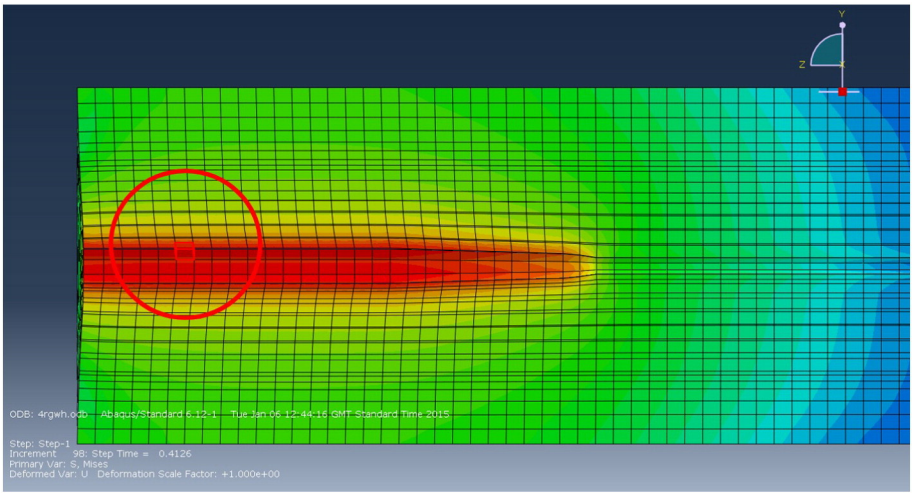

Fig. 4.8. Element displacement longitudinally parallel to catheter.

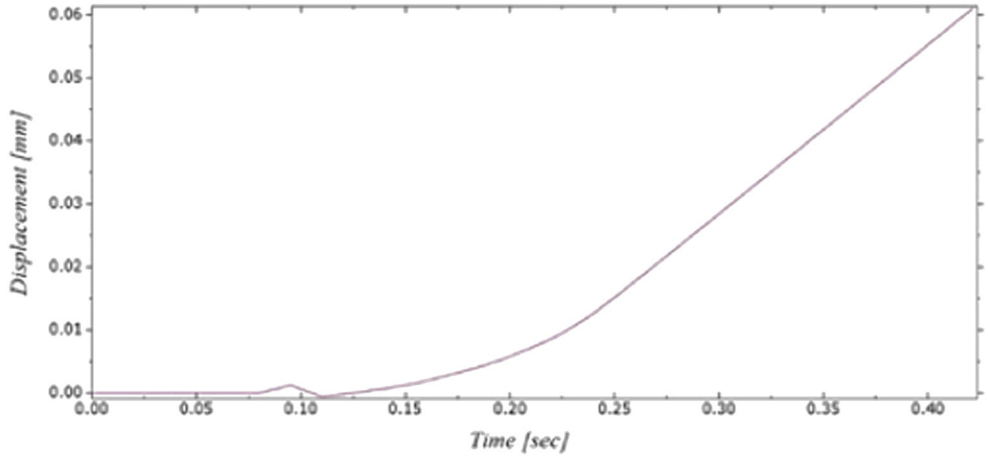

Fig. 4.9. Element displacement as a function of time.

4.6. FEA model of the urethra

Fig. 4.8 represents a FEA model of the urethra tract with a cross-sectional view containing a single element highlighted (red box). This highlighted element is used as reference point in order to measure the deflection of the urethra wall during catheterisation.

The displacement of the selected element from Fig. 4.8 is represented in Fig. 4.9 where the displacement is a function of time. The small peak at 0.1 s is a result of the catheter overcoming the static friction against the selected element. As shown in Fig. 4.9 there was an increase in the virtual urethra wall (displacement) as a simulated catheter was inserted. The numerical model utilised the frictional properties of the coating (3b) as this had the lowest coefficient of friction (0.0702) which is a desirable property needed during catheterisation. A maximum deflection of 0.06 mm over the time period of 0.5 s was predicted.

5. Conclusions

Hansen solubility parameters have been used to optimise a desired hydrophilic polymer coating for urinary catheter applications. The Tea's diagram was employed to help determine the solvent mixing ratios resulting in the development of a number of polymer–solvent homogenous solutions. It was found that the theoretical approach in determining the optimal solvent parameters was an excellent indicator in the selection of coating systems with significantly lower surface coefficient of frictions.

The SEM images illustrated how the polymer–solvent solutions were capable of producing homogenous coatings which were repeatable. It was found that the optimum coating had a thickness of 15.78 μm when the room temperature viscosity was 2.79cst. It can be seen from the FEA study that the predictions of urethra displacement can be modelled as a function of the catheters surface coefficient of friction.

Acknowledgement

This project was sponsored by the Centre of Industrial Services and Design (CISD).

References

[1] D.J. Sticker, Surface coating in urology, in: M. Driver (Ed.), Coatings for Biomedical Applications, Woodhead Publishing, Cambridge 2012, pp. 304–335.
[2] P. Sobolewski, M.E.I. Fray, Cardiac catheterization: consequences for the endothelium and potential for nanomedicine, WIREs Nanomed. Nanobiotechnol. 7 (2015) 458–473.
[3] K.H. Dellimore, S.E. Franklin, A.R. Helyer, A review of catheter related complications during minimally invasive transcatheter cardiovascular intervention with implications for catheter design, Cardiovasc. Eng. Technol. 5 (2014) 217–232.
[4] P. Parida, A. Behera, S.C. Mishra, Classification of biomaterials used in medicine, Int. J. Adv. Appl. Sci. 1 (2012) 31–35.
[5] L.C. Xua, C.A. Siedlecki, Submicron-textured biomaterial surface reduces staphylococcal bacterial adhesion and biofilm formation, Acta Biomater. 8 (2012) 72–81.

[6] N.A. Mohamed, N.A. Abd El-Ghany, M.M. Fahmy, M.H. Ahmed, Synergistic effect of maleimido phenyl urea derivatives mixed with some commercial stabilizers on the efficiency of thermal stabilization of PVC, Polym. Test. 44 (2015) 66–71.
[7] J. Stensballe, D. Looms, P.N. Nielsen, M. Tvede, Hydrophilic-coated catheters for intermittent catheterisation reduce urethral micro trauma: a prospective, randomised, participant-blinded, crossover study of three different types of catheters, Eur. Urol. 48 (2005) 978–983.
[8] J. Park, J.H. Bae, W.H. Kim, M.H. Kim, C.M. Keum, S.D. Lee, J.S. Choi, Effects of interfacial charge depletion in organic thin-film transistors with polymeric dielectrics on electrical stability, Materials 3 (2010) 3614–3624.
[9] N. Yin, S.Y. Chen, Y. Ouyang, L. Tang, J.X. Yang, H.P. Wang, Biomimetic mineralization synthesis of hydroxyapatite bacterial cellulose nanocomposites, Prog. Nat. Sci. Mater. Int. 21 (2011) 472–477.
[10] I. Eriksson, Y. Gustafson, L. Fagerström, B. Olofsson, Prevalence and factors associated with urinary tract infections (UTIs) in very old women, Arch. Gerontol. Geriatr. 50 (2010) 132–135.
[11] J. Abarbanel, D. Engelstein, D. Lask, P.M. Livne, Urinary tract infection in men younger than 45 years of age: is there a need for urologic investigation? Urology 62 (2003) 27–29.
[12] P. Ulleryd, Febrile urinary tract infection in men, Int. J. Antimicrob. Agents 22 (2003) 89–93.
[13] B. Trautner, Role of biofilm in catheter-associated urinary tract infection, Am. J. Infect. Control 32 (2004) 177–183.
[14] P.J. Stewart, J.W. Costerton, Antibiotic resistance of bacteria in biofilms, Lancet 358 (2001) 135–138.
[15] P.A. Tambyah, D.G. Maki, Catheter-associated urinary tract infection is rarely symptomatic: a prospective study of 1,497 catheterized patients, Arch. Intern. Med. 160 (2000) 678–682.
[16] S. Saint, S.R. Kaufman, M. Thompson, M.A. Rogers, C.E. Chenoweth, A reminder reduces urinary catheterization in hospitalized patients, Jt. Comm. J. Qual. Patient Saf. 31 (2005) 455–462.
[17] T. Çaykaraa, Solubility parameters of cross-linked poly(N-vinyl-2-pyrrolidone-co-crotonic acid) copolymers prepared by γ-ray-induced polymerization technique, J. Macromol. Sci. A Pure Appl. Chem. 41 (2004) 971–979.
[18] C.M. Hansen, Hansen Solubility Parameters, 2nd ed. CRC Press, Boca Raton, 2007.
[19] D.V. Krevelen, Properties of Polymers, 4th ed. Elsevier, Oxford, 2009.
[20] Y. Liu, A.E. Kerdok, R.D. Howe, A nonlinear finite element model of soft tissue indentation, in: S. Cotin, D.N. Metaxas (Eds.), Proceedings of medical Simulation, ISMS., Cambridge MA, Lecture notes in Computer Science, 3078, Springer-Verlag 2004, pp. 67–76.
[21] Z. Guo, X. Xu, Y. Xiang, S. Lu, S.P. Jiang, New anhydrous proton exchange membranes for high-temperature fuel cells based on PVDF–PVP blended polymers, J. Mater. Chem. A 3 (2015) 148–155.

Please cite this article as: B.J. Carberry, et al., Surf. Coat. Technol. (2015), http://dx.doi.org/10.1016/j.surfcoat.2015.06.029